http://www.press.ierek.com

ISSN (Print: 2357-0849, online: 2357-0857)

International Journal on:

Environmental Science and Sustainable Development

DOI: 10.21625/essd.v5i2.757

A Life-cycle Cost-benefit Analysis for Rooftop Photovoltaic Systems in Lightweight Steel-structured Industrial Buildings

Xinyi Hu[1,*], Junyu Hu[2], Hong Zhang[1]

[1] *School of Architecture, Southeast University, Nanjing 210096, China*

[2] *Department of Architecture, Civil Engineering and Environmental Sciences, TU Braunschweig， Braunschweig D-38106， Germany*

**Corrspoding author: Xinyi Hu (huxy.seu@gmail.com)*

Abstract

There is a widespread consensus that energy efficiency of buildings is an essential component of sustainable development and several kinds of renewable energy technologies have been widely used to achieve this sustainable goal. As a rapidly developing country, China's manufacturing industry still occupies a prominent position, with a large number of industrial buildings that are also a crucial part of urban planning. Compared with multi-story and high-rise commercial buildings, large industrial sheds have a much more usable roof area, where rooftop photovoltaic (PV) systems are increasingly used. However, due to the small structural margins of the lightweight steel-structured (LSS) industrial buildings and the large initial investment of the thin-film PV system, few case studies are available for this kind of industrial buildings. In this research, three representative cities in China, with varying levels of solar radiation availability, are selected as typical external design factors. Taking a typical LSS industrial building with an added thin-film rooftop PV system as an example, a life-cycle cost-benefit analysis is conducted from environmental and economic aspects. The results of the analysis demonstrate the effectiveness of the rooftop thin-film PV system as a means to increase the energy efficiency of the LSS industrial buildings.

Keywords

Industrial buildings; rooftop PV system; lightweight steel-structured; cost-benefit analysis

1. Introduction

It is well established that construction activities consume large amounts of natural resources that cause the release of carbon dioxide, entailing immense environmental load. In order to achieve energy efficient design, sustainable buildings consider the application of renewable energy technologies (Chwieduk, 2003), such as solar energy. Recent research on building integrated photovoltaic (BIPV) is mainly focused on the residential and office buildings. Industrial buildings are composed of production plants and auxiliary buildings. The auxiliary ones include warehouses and public auxiliary buildings. The sustainable development of industrial buildings also deserves attention. In 2017, China's industrial power consumption reached 4.5×10^{12} kWh, accounting for 69.4% of China's total power consumption (National Bureau of Statistics of China, 2017). According to the Green Development Plan in Industry (2016-2020), the industrial structure adjustment and the industrial transformation and upgrading promotion are mainly achieved through the transformation of traditional high energy-consuming industries and the resolution of

excess capacity (Ministry of Industry & Information Technology of China, 2016). The power efficiency retrofit of production processes and equipment, the collection and utilization of waste heat, and other relevant methods are applied to decrease the industrial power consumption.

Clean power in industry also plays a vital role in improving China's energy structure and achieving targets for saving energy and reducing emissions. Large-scale utilization of industrial plant roofs, especially the large number of light steel-structured ones, to develop distributed photovoltaic(PV) systems is a feasible and effective way to increase the proportion of clean energy generation rapidly. Compared with public buildings and residential buildings, industrial ones are mostly single-story, with low building density and large flat roofs, which means that more PV system capacity can be installed with more significant potential for solar energy applications. Industrial buildings themselves require large energy demand. China's average industrial and commercial electricity price in 2019 is $109.3/MWh, higher than the residential one of $75.56/MWh (National Energy Administration, 2017). Electricity generated by the PV systems can be employed to satisfy their own electricity demand and save power expenses. In 2017, the on-grid electricity price of PV power generation was $134.3/MWh, which was 2.5 times that of coal-fired units and 3.7 times that of hydropower (National Energy Administration, 2017). The additional generated power can also be sold to the public grid, creating new economic benefits for enterprises.

One of the factors restricting the development of rooftop PV projects in industrial buildings is the impact of the rooftop PV module weights on the roof carrying capacity, directly affecting the safety and reliability of PV projects. The total weight of conventional glass-based PV modules with brackets is about 15-20 kg/m^2, which exceeds the load margin of most lightweight steel roofs. Due to the load limitation of the lightweight steel roof, the cost of developing the rooftop PV system of the existing lightweight steel-structured industrial building and the roof reinforcement is relatively high. On the other hand, steel consumption in developing the PV system of newly-built ones is significantly affected. Given other uncertain factors, such as system installation costs and insufficient technology promotion, decision-makers still doubt the investment as it leads to few actual application cases. However, in recent years, the cost of solar cells and PV systems continues to shrink as lightweight PV module technology gradually matures (State Grid Energy Research Institute Co., 2019). The load of flexible thin-film PV panels is only 3kg/m^2, much lower than that of traditional crystalline silicon ones, which results in little impact on steel consumption. Therefore, the possibility of rooftop PV system application in lightweight steel-structured industrial buildings is steadily increasing.

The objective of this study is the typical single-story lightweight steel-structured industrial building. The main goal is to study the difference in life cycle carbon emissions of the objective building before and after the rooftop PV system installation, and the economic cost-benefit analysis of the PV system. Through the quantificational calculation of cost and gain from the environmental and economic perspective, this paper provides reasonable suggestions for the application of rooftop PV projects in industrial buildings.

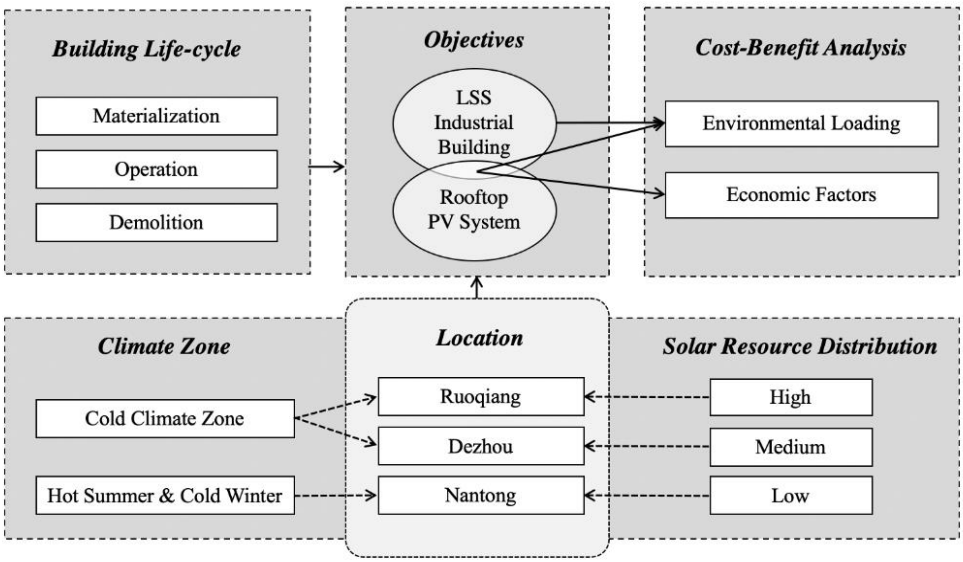

Figure 1 The research structure.

2. Methodology

The research conducted in this paper is a two-step procedure: (1) the design properties of the reference building should be decided (Section 2.1), and three cities with high, medium, and low solar energy resources respectively are chosen according to the climate context (Section 2.2); (2) before and after the rooftop PV system is installed, the life cycle carbon assessment of the industrial buildings in these three cities and life cycle economic cost-benefit of the PV system is calculated (Section 2.3 & 2.4). The research structure is depicted in Figure 1.

2.1. The reference scenario

A reference scenario was set up for further comparative analyses, considering a building featured by basic properties. The reference object is a single-story lightweight portal framed industrial building with no crane (Figure 2), the lifespan of which is assumed to be 20 years. The typical plan is 60 m×30 m, with a gross area of 1800 m^2. The top height of the outer longitudinal wall is about 5.5 m, and the highest point is 7.5 m. According to functional requirements, the column spacing of the long side is 10 m, and the portal frame span is 30 m. The independent foundations under columns are adopted. The steel beams and columns are H-shaped steel with variable cross-section.

The building is a new industrial building so that its thermal design and indoor design temperature of heating and cooling would meet the requirements of "Unified standard for energy efficiency design of industrial buildings"(MOHURD, 2017). The envelope adopts a combination of double-layer steel decks and rock wool insulation boards. The reference scenario includes the life-cycle phases evaluated using the following design conditions shown in Table 1.

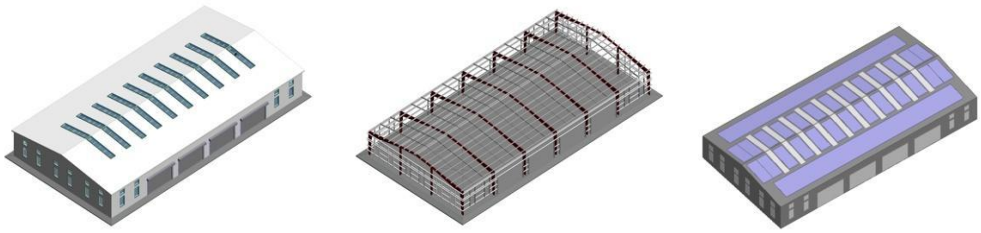

Figure 2 The envelope, structure, and simulation model of the reference building.

Table 1. Basic properties of the reference building.

Construction	Structure		Lightweight steel structure (LSS)
	Height		5.5-7.5m
	Shape coefficient		0.24
	External wall U-value		0.607 [W/m^2 K]
	Roof U-value		0.533 [W/ m^2 K]
Opening	Window ratio*	External walls	0.08
		Roof	0.12
	External windows glazing type		Clr 6+13A+6 (Aluminium window frame without break)
	Glazing U-factor		2.71 [W/m^2 K]

Table 1 Continued

HVAC	Heating system type / energy resource		Central heating / Anthracite-fired cogeneration, combined heat and power (CHP) units
	Cooling system type / energy resource		Distributed air-conditioners / Electricity
	Environmental Control	Heating set point	16 [°C] or 60.8 [°F]
		Cooling set point	28 [°C] or 82.4 [°F]

** Window ratio of external walls = Area of transparent components of external walls/ Total area of external walls ; Window ratio of roof = Area of transparent components of the roof / Total area of the roof.*

2.2. City selection

Due to various geographical locations, solar radiation intensities in China are quite different. In general, the total annual solar radiation in the western region is higher than that in the eastern region, except for Tibet and Xinjiang, and is lower in the south than in the north. Since most southern areas are foggy and rainy, located between the 30-40° north latitude, solar radiation decreases with latitude decline (Solar GIS, 2019; Tschopp et al., 2020). There are roughly five different districts in China, divided according to the amount of solar radiation (Zheng and Yi, 2010). Solar district I has the most abundant solar energy resources, the highest value located in the Qinghai-Tibet Plateau with a radiation amount higher than 2,200 kWh/m^2·yr. The lowest value is found in the Chuan-Yu region of Solar district V, with about 950 kWh/m^2·yr (Li et al., 2014).

There are five major types of climatic regions in China, which are severe cold regions, cold regions, hot summer and cold winter regions, hot summer and warm winter regions, and temperate regions, and there are different building design requirements for different climatic regions (Huo et al., 2017). Most areas of the Solar district I, II and III with abundant solar energy resources belong to severe cold and cold climate areas, while Solar district IV and V belong to hot summer and cold winter regions, hot summer and warm winter regions, and temperate regions. Most of China's areas and populations are concentrated in the Solar district II, III and IV. In this study, three representative cities are selected, namely Ruoqiang in Xinjiang in Solar district II, Dezhou in Shandong in Solar district III, and Nantong in Jiangsu in Solar district IV.

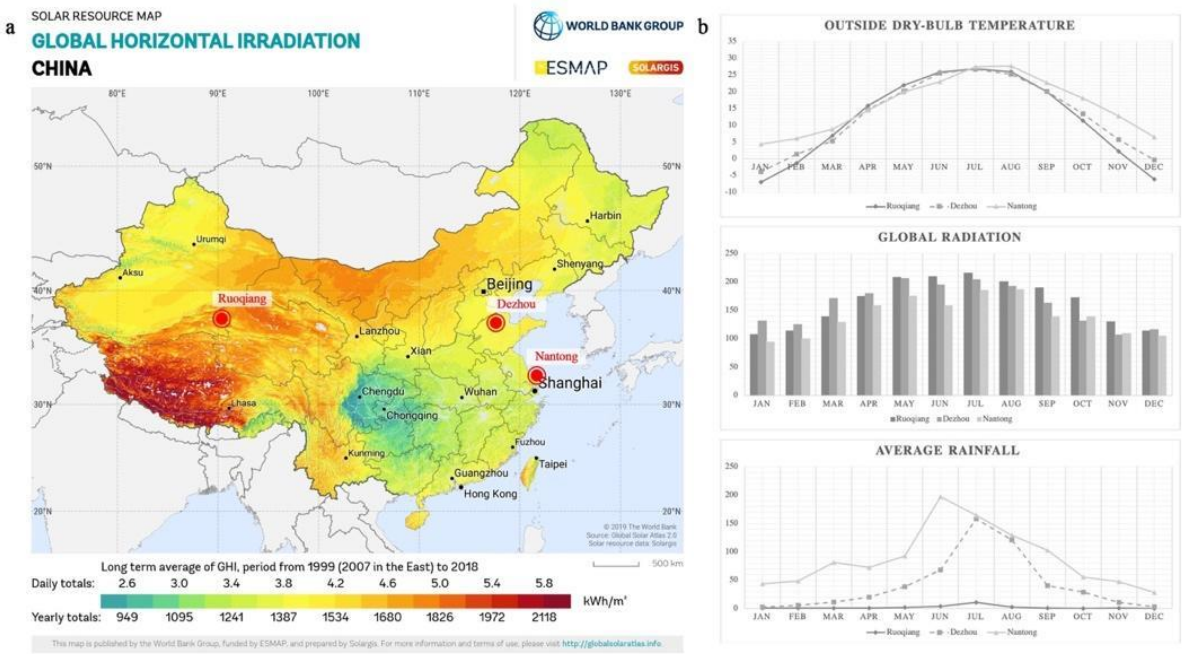

Figure 3 (a) Global irradiance in China and selected cities (Solar GIS, 2019); (b) Outside dry-bulb temperature, global radiation, and average rainfall of Ruoqiang, Dezhou, and Nantong (EnergyPlus, 2005; Weather Atlas, 2020).

The seismic design requirements and basic wind and snow loads of these three cities are similar. Therefore, the difference in the amount of steel consumption for lightweight steel-structured industrial buildings can be ignored, and these cities can be used as the design contexts. The geographical location, solar energy resources and climate conditions of the selected cities are shown in Figure 3. Ruoqiang and Dezhou belong to the cold region, while Nantong belongs to the hot summer and cold winter region.

2.3. Life Cycle Carbon Emissions Assessment methodology

Life Cycle Carbon Emission Assessment ($LCCO_2A$) considers all the carbon-equivalent emission output from a building during all five phases: materialization, transportation, on-site construction, operation, and end-of-life. The carbon emissions during raw material extraction, transportation and component manufacture period are defined as the carbon emissions during materialization period. The transportation phase in this paper consists of two processes: transporting building materials from the factory to the construction site and transporting the demolition waste from the site to the recycling factories or landfill. The end-of-life phase includes three parts, demolition, recycling, and disposal. The disposal phase is to transport the demolition waste which has been included into the calculation of the transportation phase. There is a lack of data on construction and demolition of industrial buildings, the carbon emissions which only share a little part according to the previous study (Bonamente and Cotana, 2015), so the calculation of these two stages is ignored in this paper. Therefore, $LCCO_2A$ of industrial buildings in this research is simplified as the following:

$$CO_2 = CO_{2_{Materialization}} + CO_{2_{Transportation}} + CO_{2_{Operation}} - CO_{2_{Recycling}} \quad (1)$$

where CO_2 represents the carbon emission of the whole life cycle of a building ($kgCO_2e$), $CO_{2_{Materialization}}$, $CO_{2_{Transportation}}$, and $CO_{2_{Operation}}$ represent the carbon emissions during the materialization, transportation, and operation ($kgCO_2e$), respectively. $CO_{2_{Recycling}}$ is the carbon credits obtained from recycling ($kgCO_2e$).

2.3.1. Materialization phase analysis

During the materialization phase, the amount of carbon emissions includes not only the fossil carbon emissions released during the extraction, transportation and manufacture stages, but also the process carbon emissions resulting from the chemical effects, especially the concrete manufacturing. The amount of carbon released during this phase can be determined directly as:

$$CO_{2_{Materialization}} = \sum_{1}^{i} \rho_i m_i \quad (2)$$

where ρ_i is the carbon emission factor for the i^{th} type of building material ($kgCO_2$ e/unit), which can be extracted from an appropriate carbon emission database considering both fossil and process carbon emissions (MOHURD, 2019). m_i is the amount of the i^{th} type of building material (kg or m^3), which can be summarized from the component list of the Revit model. The weight of connecting parts is estimated as the 10% of the steel.

2.3.2. Transportation phase analysis

The transportation phase is divided into two parts, the process when the building materials are transported from the factories to the construction site and the process of the demolished remains transported to the landfill and recycling site. The shipping distance applies the default values in the *Standard for building carbon emission calculation (GBT51366-2019)* (MOHURD, 2019).

$$CO_{2_{Transportation}} = \sum_{1}^{i} m_i D_i \varphi + \sum_{1}^{j} m_j D_j \varphi \quad (3)$$

where m_i the amount of the i^{th} type of building material used for construction (kg). m_j is the amount of j^{th} disposed or recycled material. D_i is the transportation distance of the i^{th} type of building material (km). The default value for

concrete is 40km, and 500km for other materials. D_j is the transportation distance between the construction site and landfill or recycling factory of the j[th] type of building material (km). For the steel, aluminium and concrete which are assumed for recycling, D_i is equal to D_j. As for the other disposed materials, D_j is assumed as 200km. φ is the carbon emission factor for transportation [kgCO_2e/(t·km)]. In this research, the value is assumed as 0.129 [kgCO_2e/(t·km)] by heavy-duty diesel trucks with load capacity of 18t.

2.3.3. Operation phase analysis

The energy consumption required for different industrial activities varies a lot. Therefore, in this study, the carbon balance during operation phase only considers emissions from minimum space heating and cooling requirements and credits from electricity generated by the rooftop PV system and Combined heat and power (CHP):

$$CO_{2_{Operation}} = T \times (CO_{2_{heating}} + CO_{2_{cooling}} - CO_{2_{CHP,elec}}) - \sum_{1}^{t} CO_{2_{PV}}(t) \quad (4)$$

The annual primary energy consumption and generation are simulated by *DesignBuilder*, based on *EnergyPlus*, where the labor intensity level inside the building is assumed as light labor (DesignBuilder Software Ltd, 2020). Both the indoor design temperature and mechanical ventilation setting meet the current design standard (MOHURD, 2017). The annual carbon emissions and credits during this phase are determined by multiplying the quantity of energy resources (coal or electricity) with its carbon-equivalent emission factor:

$$CO_{2_{heating}} = \rho_{coal} E_{heating} \quad (5)$$

$$CO_{2_{cooling}} = \rho_{elec} E_{cooling} \quad (6)$$

$$CO_{2_{CHP,elec}} = \rho_{elec} E_{CHP,elec} \quad (7)$$

$$CO_{2_{PV}}(t) = \rho_{elec} E_{pv} \eta_{PV} \sigma(t) \quad (8)$$

Where $CO_{2_{heating}}$ and $CO_{2_{cooling}}$ represent the annual carbon emissions due to the heating and cooling system (kgCO_2e/yr). $CO_{2_{CHP,elec}}$ is the annual carbon credits from the CHP unit (kgCO_2e/yr), while $CO_{2_{PV}}(t)$ is the carbon credits from the electricity generated from the PV system in the t[th] year (kgCO_2e). T is the building life span and is assumed as 20 years in this study. $E_{heating}$ and $E_{cooling}$ are the annual energy consumption due to heating and cooling demand (kWh/yr). $E_{CHP,elec}$ is the annual amount of power generated from the CHP units (kWh/yr). E_{PV} is the theoretical amount of electricity generated by the PV system (kWh/yr). η_{PV} is the efficiency of the generation system considering losses due to conversion and dirt, which is summarized as 89.3%. $\sigma(t)$ is the solar module efficiency in the t[th] year, which is 97% in the first year and decays at a rate of 0.7% every year until the end of use. T is the lifespan of the building, assumed to be 20 years in this study. ρ_{coal} and ρ_{elec} are the carbon emission factor of anthracite and electricity grid, with the value as 0.34 kg CO_2e/kWh and 0.9914 kg CO_2e/kWh, respectively.

2.3.4. Recycling phase analysis

The credits during recycling are calculated as the emission difference between the original production and reproduction after recycling.

$$CO_{2_{Recycling}} = \sum_{1}^{j} (1 - \alpha_j)\omega_j CO_{2_{Materialization,j}} \quad (9)$$

Where α_j is the ratio of carbon emissions between the reproduction and the original production of the j[th] building materials, calculated as 50% (MOHURD, 2019). $CO_{2_{materialization,j}}$ and ω_j are the carbon emissions during materialization and recycling rate of the j[th] recycled material. According to the previous study, the recycling rate of the steel, rebar in concrete, and aluminum are estimated as 90%, 50%, and 95% (Yan, 2011).

2.4. Cost-Benefit Analysis of the PV system

The two-slope roof is loaded with a flexible thin-film PV system of 128.4kW. Its economic cost-benefit analysis, similar to the aforementioned LCCO$_2$A, includes three phases: the initial investment phase, the operation phase, and the demolition phase. There are obvious investment and income variables in the first two stages, and the third one is the estimated cost of dismantling and recycling after 20 years. Considering that this project is a distributed PV project with a small installed capacity, and currently China's PV panel recycling technology is not mature enough, the calculation of the third phase is eligible in this study. Therefore, the cost-benefit analysis of the PV system can be based on the following formula:

$$B_{PV} = \sum_{1}^{t} B_{op}(t) - C_{op} - C_{invest} \tag{10}$$

Where B_{PV} is the total benefit of the rooftop PV system during the 20-year life cycle (\$), C_{invest} is the initial investment, C_{op} and B_{op} are the cost and benefit during the operation phase (\$).

2.4.1. Initial investment

The initial construction costs include the equipment procurement cost, design and installation fees, and other sub-charges. It is generally calculated by multiplying the installed capacity by the cost per unit of installed capacity:

$$C_{invest} = W \times C_w \tag{11}$$

Where W is the installed capacity of the PV system (kW). C_w is the unit cost of the system (\$/W), which is the summarized cost of the sub-items in Table 3.

Table 2. Cost breakdowns of the industrial distributed PV system (Manman, 2019; Patel, 2020)

Sub-item	**Cost (\$/W)**	**Category**	**Sub-item**	**Cost (\$/W)**	**Category**
Solar module	0.650	Equipment procurement	Design fee	0.029	Design
Inverter	0.055		Engineering insurance	0.007	Installation and debugging
Combiner box	0.017		System debugging	0.017	
DC/AC cable	0.036		Installation fee	0.080	
Monitoring system	0.043		Others	0.014	
Total	0.948				

2.4.2. Cost and benefit during the operation phase

The system's operation cost includes annual maintenance and insurance fees, as well as the replacement cost of the inverter in the 10th year. The self-generation of power is firstly supplied for self-use, and surplus power is sold to the public grid. The benefits are divided into three parts: state subsidies for PV power, the cost savings of self-use electricity, and the revenue of on-grid surplus power.

$$C_{op} = T \times C_{invest} \times (\beta_m + \beta_{insur}) + C_{invest} \times \beta_{inver} \tag{12}$$

$$B_{op}(t) = P_{sub} \times \sum_{1}^{t} E_{PV}\eta_{PV}\sigma(t) + P_x \times T \times E_{cooling} + P_y \times \sum_{1}^{t} \left[E_{PV}\eta_{PV}\sigma(t) - E_{cooling}\right] \tag{13}$$

β_m, β_{insur}, and β_{inver} represent the system maintenance rate, insurance rate, and inverter replacement rate, which are 1.20%, 0.25%, and 8.56%, respectively. P_{sub}, P_x, and P_y are the state subsidy, general industrial electricity price, and feed-in tariffs for PV power in Ruoqiang, Dezhou, and Nantong, the value of which are presented in the Table 4.

Table 3. The state subsidy, industrial electricity price, and on-grid price of PV generation in three typical cities.

	General industrial electricity price ($/kWh)	**Feed-in tariffs for PV power ($/kWh)**	**State subsidy ($/kWh)**
Ruoqiang	0.066	0.057	0.014
Dezhou	0.094	0.064	
Nantong	0.100	0.079	

3. Results and Discussion

3.1. Results of the Life Cycle Carbon Emissions Assessment

In this paper, process-based analysis is applied to obtain detailed results presented in Figures 4-6, respectively. The embodied carbon amounts and distribution of each raw material for the reference building are presented in Table 4 and Figure 4. 1136 tons of concrete is used to construct the building, which corresponds to about 89% of the overall weights of the building. Most of the embodied carbon emissions are contributed from steel with five types (50.04%), concrete (30.70%), and mineral wool (14.53%), and the remaining is the materials used for skylights and windows. The higher amount of embodied carbon for steel and concrete compared to other materials is due to the larger volume of steel and concrete. Electrolytic aluminum is a high-carbon emission industry. However, due to the low density of aluminum, the total weight of the aluminum window frames used is small and its carbon emissions only account for 0.03%.

Table 4. The embodied carbon emissions of different materials used in the reference building.

Components	**Type of building material**	**Mass (kg)**	**Carbon emissions ($kgCO_2$ e/m^2 floor)**
Columns, beams, wind columns	Hot-rolled carbon H steel	32734.50	42.74
Column bracing and roof horizontal bracing	Hot-rolled carbon steel bar	5573.50	7.25
Purlins	Cold-rolled carbon steel coil	14836.50	20.85
External walls and roof, shutter doors	Hot-galvanized carbon steel coil	26974.58	46.61
Independent foundations	Hot rolled carbon steel rebar	1470.90	1.91
-	Connecting parts	5314.45	7.08
Independent foundations and the floor with apron	Concrete - C30	1135752.00	77.56
Skylights and windows	Aluminum	7.45	0.08
	Glass	18939.60	11.89
Insulation material	Mineral wool board	33364.13	36.70

Note: The density of mineral wool board used in the reference building is 180 kg/m^3 .

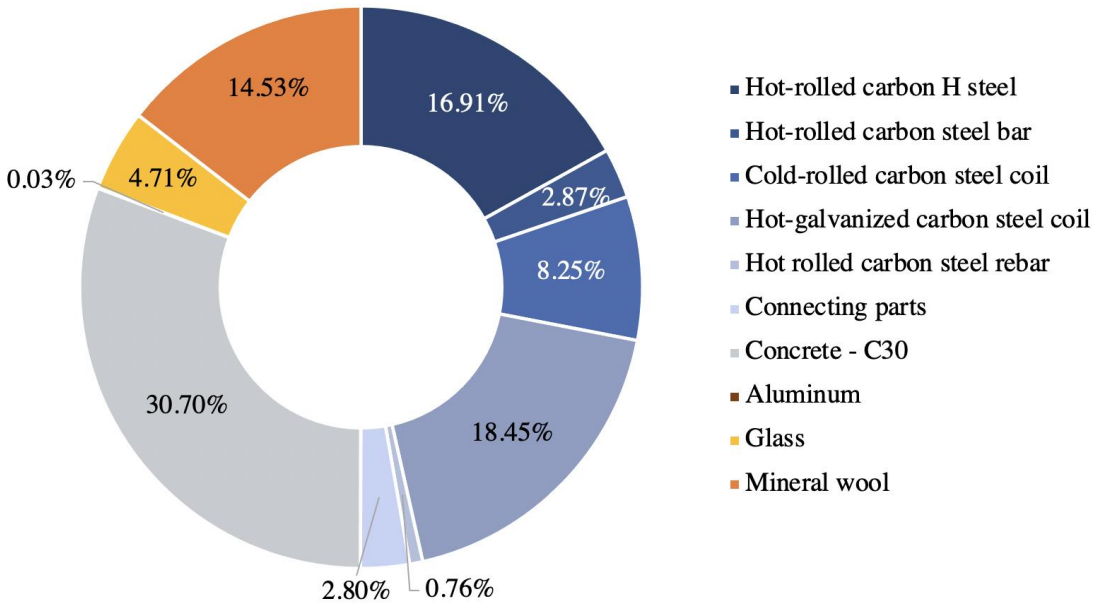

Figure 4 Carbon emissions of different materials used during the production phase.

The heating demand is satisfied by the anthracite-fired CHP units with heat and power production simultaneously, offering a number of environmental benefits over traditional heating methods, particularly other fossil fuels. As shown in the below Figure 5 and Figure 6, Ruoqiang and Dezhou are located in the cold region, with the annual heating demand and CHP power generation higher than that of Nantong. This latterre is located in hot summer and cold winter regions, where the carbon emissions increase significantly in July and August due to cooling devices. For these three cities, the carbon credits obtained from CHP generation are smaller than carbon emissions during winter months (from January to March and from October to December). No heating demand in other seasons means that there is no extra carbon credit from CHP generation. But with the PV system installed, as shown in Figure 6, the buildings will gain carbon credits all year around. The monthly carbon credits obtained from CHP and PV generation are even bigger than carbon emissions from heating or cooling.

Figure 7 presents the life-cycle carbon balance of the reference buildings with or without the PV systems in three typical cities. Due to climate differences, the carbon emissions during the operation phase vary a lot in the three cities. The proportion of carbon emissions during materialization, transportation, and operation is 11.71%, 0.71%, and 87.57%, respectively in Ruoqiang. This proportion is 13.97%, 0.85%, and 85.18% in Dezhou. While it changes to 24.34%, 1.48%, and 74.18% in Nantong. Without the PV system, the carbon emissions in three cities are all bigger than credits from CHP generation. If the PV system is installed, the buildings will be converted into more environmentally friendly ones. The carbon balance is achieved by PV power generation alone, with the values of 2222 $kgCO_2e/m^2$, 1999 $kgCO_2e/m^2$, and 1706 $kgCO_2e/m^2$ in Ruoqiang, Dezhou, and Nantong.

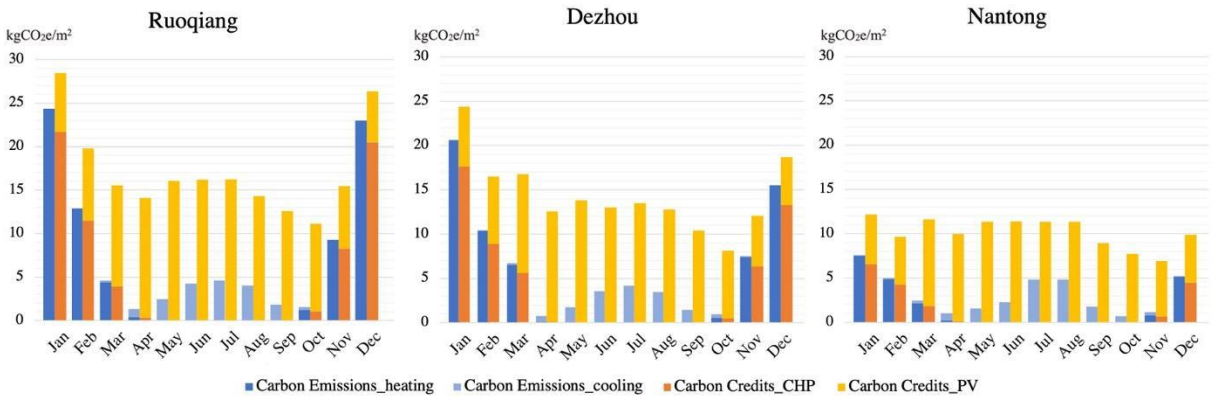

Figure 5 Monthly carbon emissions and credits during the operation phase.

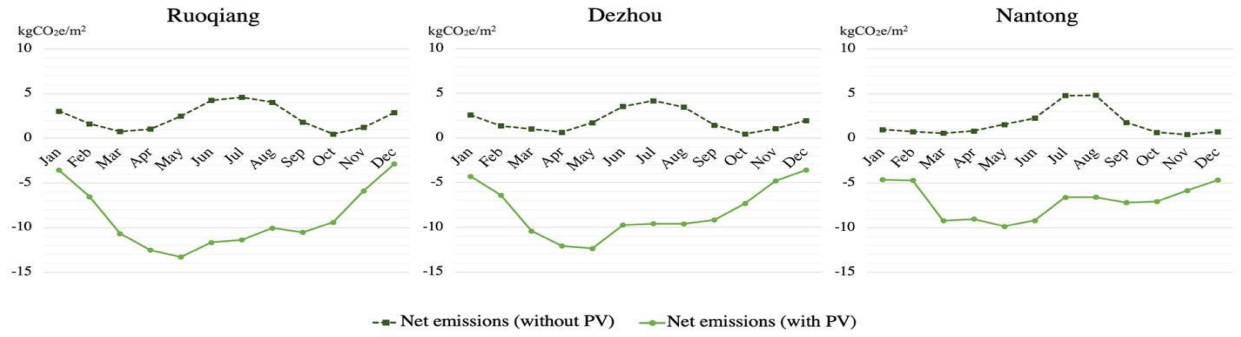

Figure 6 Monthly net carbon emissions during the operation phase.

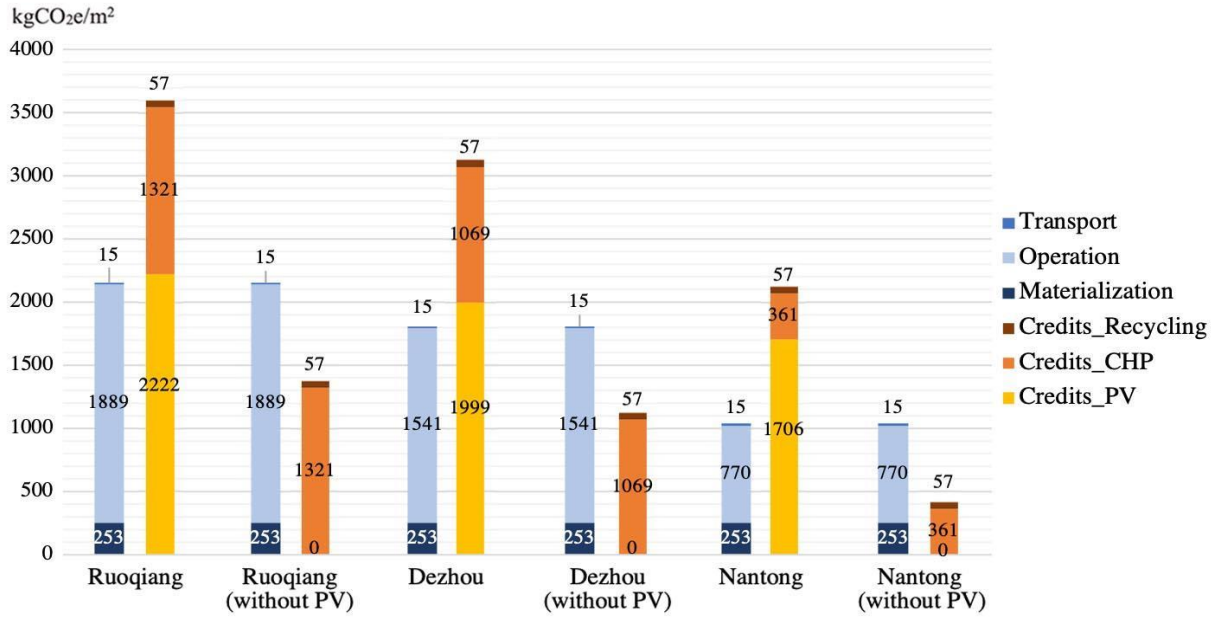

Figure 7 Life-cycle carbon balance of the buildings with or without PV systems.

3.2. Cost-benefit analysis of PV system

Taking into account the decay rate of PV systems, the actual total power generation of the buildings in Ruoqiang, Dezhou, and Nantong within 20 years is 4000MWh, 3599MWh, and 3071MWh, respectively. Figure 8 shows the distribution of the life-cycle PV generation power and the corresponding share of revenues. The building in Nantong has the largest proportion of self-use electricity at 21.12%, with electricity savings accounting for 21.68% of the total revenue. The self-use proportion of the building in Dezhou (16.08%) is slightly smaller than that of Ruoqiang (17.21%). However, Ruoqiang's industrial electricity price is lower, resulting in the proportion of cost savings in Dezhou (18.25%) more significant than Ruoqiang (15.66%).

During the whole life-cycle, the annual cumulative cost and benefits are shown in Figure 9. The initial investment is \$121,723. Except for the additional inverter replacement in the 10th year, the annual fixed cost during the operation period is \$1,765. The net profits of the Ruoqiang, Dezhou, and Nantong PV projects are \$122,747, \$130,621, and \$131,810, respectively. The specific costs and benefits are shown in Table 5. In the 20-year cycle, the initial investment accounts for about 72.70% of the total cost, and the profit margin is 42.30-44.05%. The net profit of PV projects was firmly related to the initial investment cost. The simple payback period of the project in Ruoqiang is 10 years, and that of Dezhou and Nantong are 9 years, which means that the revenues expend the cost or reach the break-even point at this time. The Ruoqiang area has the best solar resources among the selected cities with the largest power generation and state subsidies. However, due to the low industrial electricity price and low on-grid price of PV power, the net profit in the whole cycle is the smallest and the payback period is the longest. Therefore, the net profit of PV projects is not positively correlated with local solar radiation.

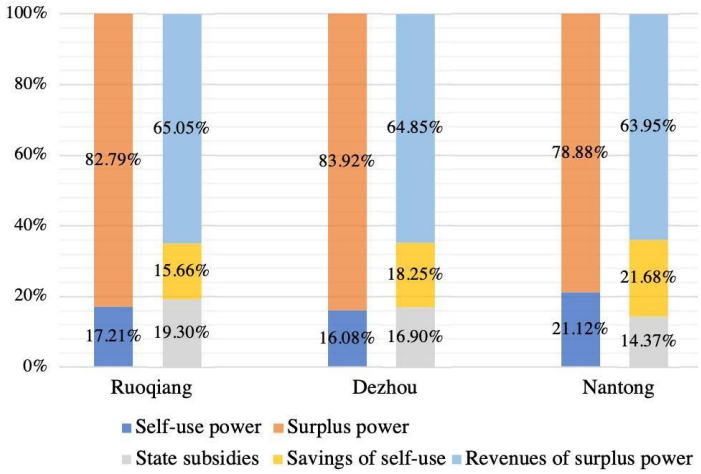

Figure 8 The distribution of the life-cycle PV generation power and revenues.

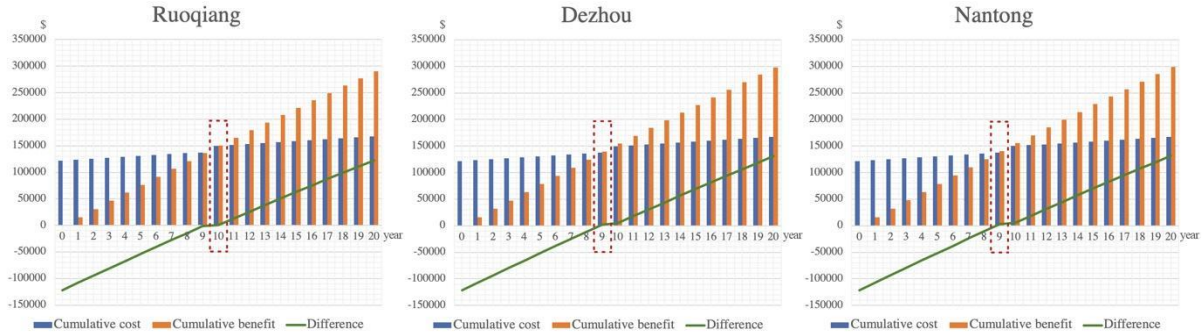

Figure 9 Annual cumulative cost-benefit analysis.

Table 5. Life-cycle cost-benefit analysis of the reference buildings in selected cities

	C_{invest} ($)	C_{op} ($)	Total cost ($)	State subsidies ($)	Savings of self-use ($)	Revenues of surplus power ($)	Gross revenues ($)	Net profits ($)
Ruoqiang	121723	45719	167442	55999	45436	188754	290189	122747
Dezhou				50383	54395	193286	298064	130621
Nantong				42998	64873	191381	299253	131810

4. Conclusion

A life-cycle cost-benefit analysis of a typical Lightweight Steel Structure industrial building is conducted. The aim of this study is to quantitatively analyze the effects of applying the rooftop thin-film PV system on this kind of buildings from both environmental and economic aspects and provide reasonable suggestions for decision-makers. In terms of environmental loading, the total carbon credits from PV systems of the reference buildings in three typical cities with different solar radiation intensities balance the carbon emissions throughout the life cycle. During the operation phase, the monthly carbon revenue generated by CHP units and PV systems is greater than the emissions due to heating and cooling. As for the absence of PV systems, the carbon revenues from the CHP production and material recycling of the reference buildings in selected cities are less than the total carbon emissions. In terms of economic benefits, the profit margin of this PV project in three cities is 42.30-44.05%, with the payback period 9-10 years. Because of the different industrial tariffs of electricity and on-grid prices of PV generation in different regions, the net profit of the project and the abundance of solar energy resources is not a positive correlation, where various influencers, such as construction environment, state policy and market price, should be considered.

Taken together, these findings suggest a positive role for the application of rooftop thin-film PV projects for the Lightweight Steel Structure industrial buildings from both environmental and economic perspectives, which provides reasonable references for decision-makers. It would be interesting to compare the environmental and economic benefits of lower-priced silicon solar panels applied to the reference building with some structural reinforcement, to those of the thin-film solar panels, as part of a future research.

References

Bonamente, E., & Cotana, F. (2015). Carbon and energy footprints of prefabricated industrial buildings: a systematic life cycle assessment analysis. *Energies*, *8*(11), 12685-12701. https://doi.org/10.3390/en81112333

Chwieduk, D. (2003). Towards sustainable-energy buildings. *Applied energy*, *76*(1-3), 211-217. https://doi.org/10.1016/S0306-2619(03)00059-X

DesignBuilder Software Ltd (2020). *DesignBuilder Software* [WWW Document]. Retrieved 6 August 2020 from https://designbuilder.co.uk/.

EnergyPlus (2005). *Weather Data by Region | EnergyPlus* [WWW Document]. Retrieved 6 August 2020 from https://energyplus.net/weather-region/asia_wmo_region_2/CHN.

Huo, Haie, Shao, J., Huo, Haibo, 2017. Contributions of energy-saving technologies to building energy saving in different climatic regions of China. Appl. Therm. Eng. 124, 1159–1168. https://doi.org/10.1016/j.applthermaleng.2017.06.065

Li, Y., Liao, S., Rao, Z., & Liu, G. (2014). A dynamic assessment based feasibility study of concentrating solar power in China. *Renewable energy*, *69*, 34-42. https://doi.org/10.1016/j.renene.2014.03.024

Manman, H. (2019). Research on the Economic Analysis and Development Policies of Distributed Photovoltaic Power Generation Project. North China Electric Power University.

Ministry of Industry & Information Technology of China (2016). *Green Development Plan in Industry* (2016-2020).

MOHURD (2019). *GBT51366-2019, Standard for building carbon emission calculation*. China Architecture Publishing & Media Co., Ltd, Beijing.

MOHURD (2017). GB51245-2017, Unified standard for energy efficiency design of industrial buildings. China Planning Press, Beijing.

National Bureau of Statistics of China (2017). *National Data*.

National Energy Administration (2017). 2017 National Electricity Price Regulatory Notice.

Patel, K., (2020). *Solar Panels Cost* [WWW Document]. Retrieved 14 August 2020 from https://solarenergyforus.com/solar-panels-cost/.

Solar GIS (2019). *Solar resource maps and GIS data for 180+ countries | Solargis* [WWW Document]. Retrieved 5 August 2020 from https://solargis.com/maps-and-gis-data/download/china.

State Grid Energy Research Institute Co. L. (2019). *China New Energy Power Generation Analysis Report (2019)*. State Grid Energy Research Institute Co., Ltd., Beijing，China.

Tschopp, D., Tian, Z., Berberich, M., Fan, J., Perers, B., & Furbo, S. (2020). Large-scale solar thermal systems in leading countries: A review and comparative study of Denmark, China, Germany and Austria. *Applied Energy*, *270*, 114997. https://doi.org/10.1016/j.apenergy.2020.114997

Weather Atlas (2020). China - Weather forecast: Detailed weather conditions and forecast, long range monthly forecast and climate data | Weather Atlas [WWW Document]. Retrieved 6 August 2020 from https://www.weather-atlas.com/en/china.

Yan, Y. (2011). Research of energy consumption and CO2 emission of buildings in Zhejiang Province based on life cycle assessment. *Zhejiang University: Hangzhou, China*.

Zheng, W., Yi, R., (2010). Utilization and development of solar energy industry in China. *Resources & Industries*, *12*(2), 89-92.